18th Brazilian Congress of Thermal Sciences and Engineering
November 16-20, 2020 (Online)

ENC-2020-0305
GEOMETRIC OPTIMIZATION OF MICROCHANNEL HEAT EXCHANGERS USING CONSTRUCTAL THEORY

Alex Maliska de Moura
Elizaldo Domingues dos Santos
Jeferson Avila Souza
Universidade Federal do Rio Grande - FURG. Avenida Itália, km 8, s/n, CEP 96203-900, Rio Grande - RS - Brazil
Email alexmaliska@hotmail.com, elizaldosantos@furg.br, jasouza@furg.br

Abstract. *This paper proposes a new methodology for microchannel heat exchangers design. It uses the basic principle of minimize flow resistance, stated by the Constructal Theory, to build the internal channels geometry. Unlikely the usual design methodologies where channel form is a predefined parameter, in this work its geometry is constructed. Flow and heat transfer problems are solved and an internal (to the channel) fin is make to evolve such as heat exchange between fluid and solid is maximized. The technique allowed to generate the geometry based on a control function and the Constructal Theory.*

Keywords: heat exchanger, Constructal Theory, numerical solution, open source solver.

1. INTRODUCTION

Energy removal is an important issue both for industrial equipment and common home devices such as computers, refrigerators and air conditioners. Many of these equipment are subjected to high energy flows and efficient heat removal is essential to maintain acceptable temperature values. The use of heat sinks serves this purpose well, acting as promoters for energy exchange between the medium to be cooled and a fluid at a lower temperature.

Microchannel heat exchangers appear to be an excellent option to meet this demand. Its construction allows a larger area of thermal exchange for the same volume construction, bringing advantages such as higher heat transfer rate, reduced refrigerant charge and reduced volume.

Aiming to better understand the potentialities of microchannel heat exchangers, many experimental and numerical works have been reported in literature. According to Qu and Mudawar, (2002a), due to its reduced dimensions, the heat transfer by conduction in the solid needs to be solved simulataneous with the heat transfer by convection in the fluid. Most of the studies concentrate in increase thermal performance of the heat exchanger by searching for optimal geometrical and operational conditions. In the work of Kawano et al., (2001), thermal efficiency and pressure drop were experimental and numerical analyzed in a heat exchanger with 70 x 57 x 180 μm channels. Similarly, in the works of Qu and Mudawar, (2002a), (2002b), heat exchanger performance was evaluated in terms of pressure drop, temperature distribution and flow characteristics (different Reynolds numbers). In terms of geometry optimization, it is possible to cite the works of Bello-Ochende et al., (2007) that investigated the optimal channel design to reduce maximum cell temperature and the work of Kou et al., (2008) which investigated thermal resistance as a function of width and height of the microchannels.

In this work, a numerical study was carried out with the objective of building a microchannel type heat exchanger. The methodology is based on the Constructal Theory Bejan, (1997), (2000) and the work of Pedroti et al., (2020), and proposes the construction of the heat exchanger from a basic form aiming to find a fin arrangement that maximizes the thermal performance.

2. PROBLEM DESCRIPTION

Geometry of the microchannel heat exchanger is shown in Fig. 1. It represents a large channel on which the fins are added according to building process described in section 2. The heat exchanger has external dimensions W = 1 mm, H = 0.36 mm and L = 10 mm while the internal channel has w = 0.97 mm and h = 0.18 mm.

Thermal and fluid flow problems, in both solid and fluid regions, are solved simultaneously using OpenFOAM software Weller et al., (n.d.). Geometry creation and discretization was performed with GMSH Geuzaine and Remacle, (2009) and post process using ParaView (Ayachit, 2015).

Mathematical model includes energy equation for both solid and fluid regions and continuity and momentum equations for the fluid region. Flow is assumed laminar, incompressible with constant physical properties. It is worth

mentioning that the thermophysical properties are constant and not significantly affected by temperature difference in the domain. Therefore, the buoyancy forces are neglected in the present problem. Thus, in the fluid region, the mathematical model is given by

$$\nabla \cdot \vec{v} = 0 \tag{1}$$

$$\rho\,(D\vec{v})/Dt = -\nabla p + \mu\nabla^2\vec{v} \tag{2}$$

$$\rho c\; DT/Dt = k\nabla^2 \cdot T \tag{3}$$

where $\vec{v}$ is the velocity vector [m/s], t the time [s], p the pressure [Pa], ρ the fluid density [kg/m³], μ the viscosity [Pa.s], c the fluid specific heat [J/kg K], k the fluid conductivity [W/m K], D the material derivative, $\nabla$the gradient operator and $\nabla \cdot$ the divergent operator.

For the solid region, energy equation can be written as

$$\rho_s c_s \partial T/\partial t = k_s \nabla^2 . T \tag{4}$$

where T is the temperature [K], and s sub index in physical properties indicates solid.

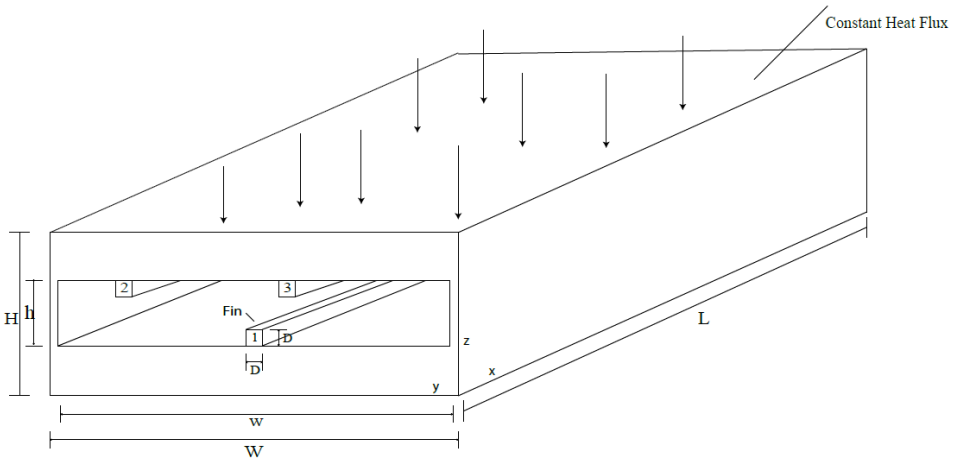

Figure 1. Computational domain.

Fluid flow boundary conditions are prescribed inlet volumetric flow rate (Q = 2.8x10^{-7}m³/s), representing Re = 484 for the empty channel, prescribed pressure (p = 0 Pa) at the outlet section and no slip at the walls. For the thermal problem, prescribe temperature is specified at inlet section (T = 293 K), full developed flow ($\partial T / \partial x = 0$) at the outlet section, prescribed flux (q" = 9x10^5 W/m^2) at the top wall and insulated external walls.

2.1. Solution algorithm

The construction algorithm proposed by Vianna et al., (2018) is used here to control the fin creation inside the heat exchanger channel. Fins are sequentially added to the channel (see numbers in Fig. 1) up to the maximum temperature in the domain no longer decrease. This algorithm, which for brevity reasons will not be repeated here, has nine steps and was already applied to a similar problem in the work of Pedroti et al., (2020). Main idea is to solve the thermal problem and based on results determine the location where the new fin should be positioned. This procedure is repeated for every new fin addition.

For the positioning of the fins, a construction function is used. This function indicates, based on the velocity and temperature fields, the best place for the positioning of the solid material in the channel. This is the location where higher heat transfer rates between solid and fluid will are expected to occur. This control function is defined as

$$\phi = U/U_{max} \,.\, T/T_{max} \tag{5}$$

where U is the velocity magnitude vector [m/s] and the sub index max indicates the maximum values of the variables in the domain

Some constraints must be defined in order to solve the problem. The internal channel has fixed cross section area (w x h) and constant length L. In this solution, dimensions of the construction fins are also fixed to D x D x L, where D is equal to 0.043mm. Some restrictions are also applied for the positioning of the fins: they cannot be built where there is no support, or where their dimensions occupy the space of another fin.

Computational domain creation and discretization was obtained with GMSH software while numerical solution was performed with a finite volume solution using OpenFOAM software. Main control solution parameters are presented in Tab. 1.

Table 1 - OpenFOAM control parameters.

Variable		Parameter	
Software version		7.0	
Algorithm		PIMPLE	
Solver		chtMultiRegionFoam	
Interpolation Schemes		**fluid**	**solid**
Transient		Euler	Euler
Gradients		Gauss linear	Gauss linear
Laplacian(alpha,h)		-	Gauss linear corrected
Divergent			
	div(phi,U)	Gauss upwind	
	div(phi,h)	Gauss upwind	

3. VERIFICATION

First study case relies on the validation of the current CFD (Computational Fluid Dynamics) solution. The work of Kawano et al. (2001) has been reproduced and results are compared. The problem geometry and discretization are shown in Fig. 2. Boundary conditions are the same discussed in section 1, however only one microchannel is solved. A constant heat flux of $q'' = 9 \times 10^5$ W/m² was specified at the top solid wall and the inlet temperature was set to $T_\infty = 293$ K. Velocity at the inlet section was adjusted to represent five flow conditions (Re = 90, 140, 200, 300 and 400). Solid parts are made of silicon with thermal conductivity $k_s = 148$ W/m K, specific heat $c_s = 712$ J/kg K and density $\rho_s = 2330$ kg/m³. Working fluid is water with $Pr = 7$, specific heat $c = 4179$ J/kg K, viscosity $\mu = 1 \times 10^{-3}$ Pa s and density $\rho = 998$ kg/m³.

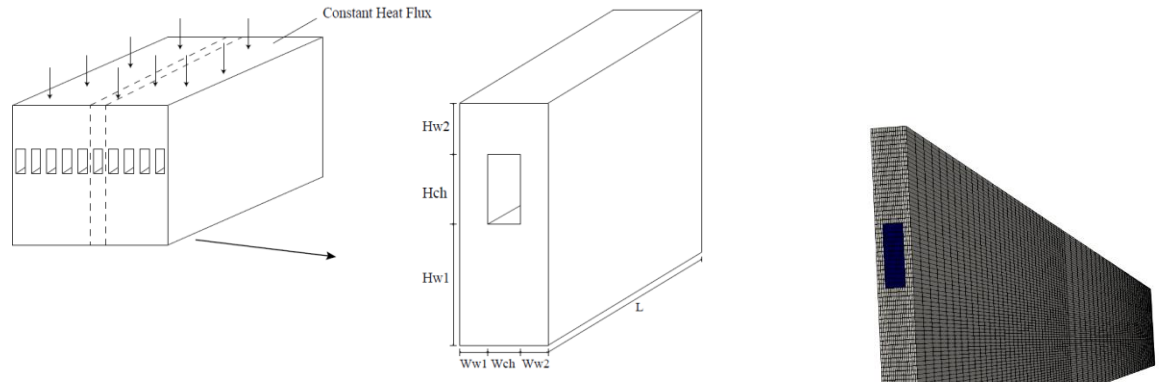

Dimensions of unit cell of micro-channel heat sink

Ww1 (μm)	Wch (μm)	Ww2 (μm)	Hw1 (μm)	Hch (μm)	Hw2 (μm)	L (mm)
21.5	57	21.5	450	180	270	10

(a) (b)

Figure 2. Model adapted from Kawano et al., (2001): a) geometry, b) discretized.

An independence grid test was performed and a domain with 122300 volumes was used to solve the problem.

Independent grid is shown in Fig. 2b where it can be verified that grid is more refined in the fluid region and closer to the inlet section.

Numerical solution obtained with the independent grid is compared with the numerical results presented by Kawano et al., (2001). Thermal resistance, given by

$$R = (T_{max} - T_{\infty})/q'' \tag{6}$$

was used in the comparison. In Eq. (6) T_{max} is the maximum temperature in the domain.

Figure 3 shows that present solution reproduces with good qualitative agreement the results reported by Kawano et al. (2001). Maximum difference of 19.4% was observed for Re = 90 while for all other runs it remained below 4.6%.

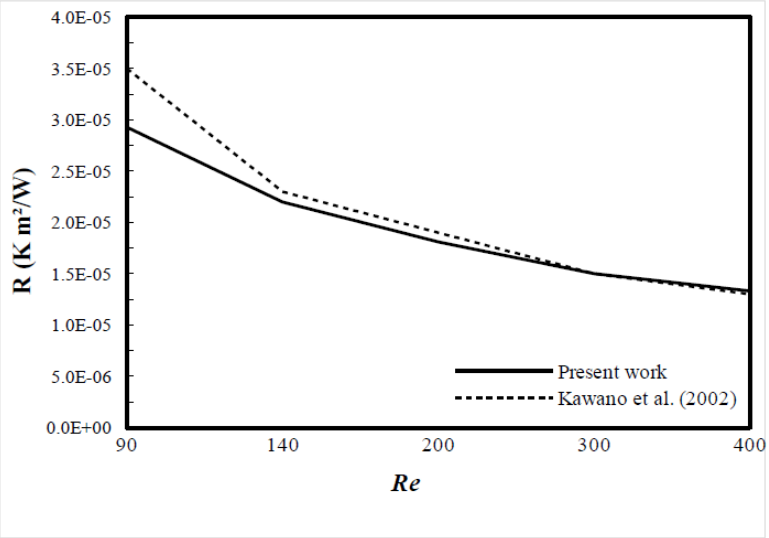

Figure 3. Verification of the numerical solution.

Temperature distribution at the mid section of the computational domain for different Reynolds numbers are shown in Fig. 4. Due to the difference in temperature fields between the solid and liquid regions, the channel can be easily identified. The temperature decreases from the top (wall subjected to the heat flux) to the bottom of the heat exchanger, with fluid regions always at a lower temperature than the solid regions. Maximum temperature is always observed at the intersection edge between top wall and outlet section of the computational domain.

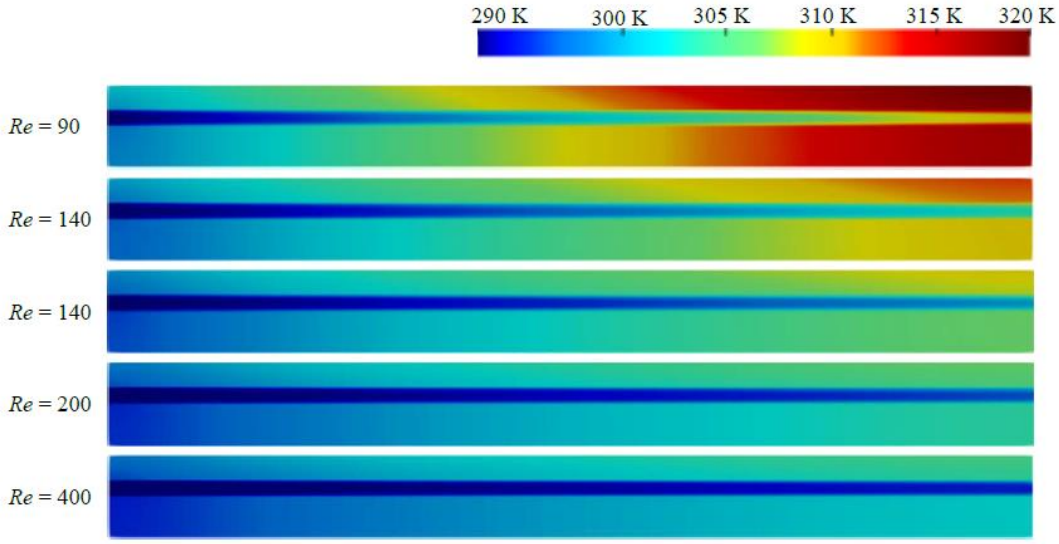

Figure 4. Temperature profiles along the mid section of the computational domain for different Re.

As can be seen in Fig. 4, the Reynolds number strongly effects the thermal behavior inside the heat exchanger. For lower Re, temperatures are higher for both fluid and solid, mainly close to the end (outlet) of the microchannel. In the temperature fields of Fig. 4, for Re = 90, maximum temperature is approximately 319 K, while for Re = 400, the maximum

temperature is about 306 K. Optimal temperature determination depends on the relationship between pressure drop and the desired maximum temperature values. As pressure drop is determined by the viscous friction with the channel walls, and increases according to the velocity, it directly interferes with the pump power needed to keep the fluid circulating.

4. RESULTS

In this section, computational domain and flow conditions described in Problem Description section are used to build the internal geometry of the microchannel heat exchanger.

Figures 5 and 6 show the first two steps of the geometry construction process. After flow and thermal problems solution for the empty channel (no fins), control function ϕ is evaluated at outlet section of the channel. This is the section where the greatest temperature gradients are observed and fluid flow is fully developed. In Fig. 5, the white star indicates the coordinates (x_{cf}, y_{cf}, z_{cf}) where ϕ is maximum. For the first solution step, it is at the center of the channel. Numerical value of the control function variable has no physical meaning, thus no legend is provided for the ϕ fields plotted in Figs. 5 and 6.

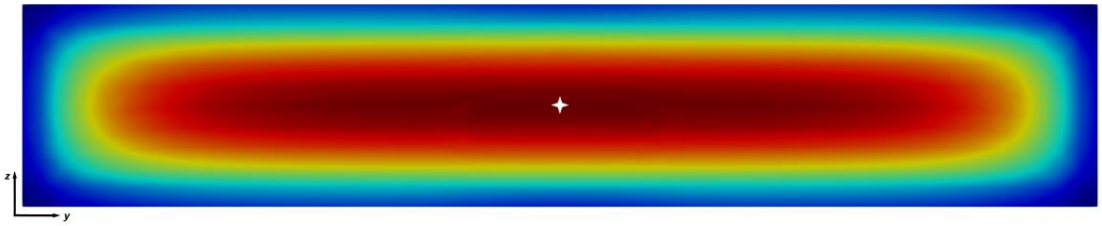

Figure 5. Point where the center of the first fin will be placed according to the control function ϕ.

First fin is positioned at the y_{cf} coordinate and extended from the top wall (nearest solid wall) up to the z_{cf} coordinate, as can be seen in Fig. 6.

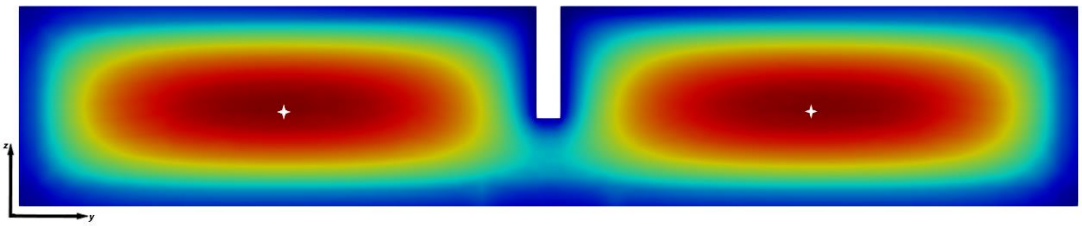

Figure 6. First fin positioned and points where the next fins will be placed.

Again, after solving the velocity and temperature fields for the second configuration, the second fin location is determined. Due to the symmetry of the problem, there are actually to locations where ϕ is maximum. These locations are represented by two white stars equidistant from the channel center in Fig. 6. It is also noticed that, for the used construction function (see Eq. (6)), the velocity has a greater influence than the temperature in the positioning of the fins, since in the locations where its value is higher, an equally high value of ϕ is observed. The process continues successively until the geometry shown in Fig 7 is obtained. In Fig. 7 the numbers indicate the sequence in which each fin was added to the domain.

Figure 7 shows the velocity field at the entrance of the channel. The high velocity value at the center indicates that this location would be a likely place of a new fin. However, after this configuration, there were practically no changes in the maximum temperature values in the domain, indicating a loss of efficiency in the thermal exchange, possibly caused by the greater flow restrictions that new fins would cause. The gray region in Fig. 7 represents the solid part of the heat exchanger.

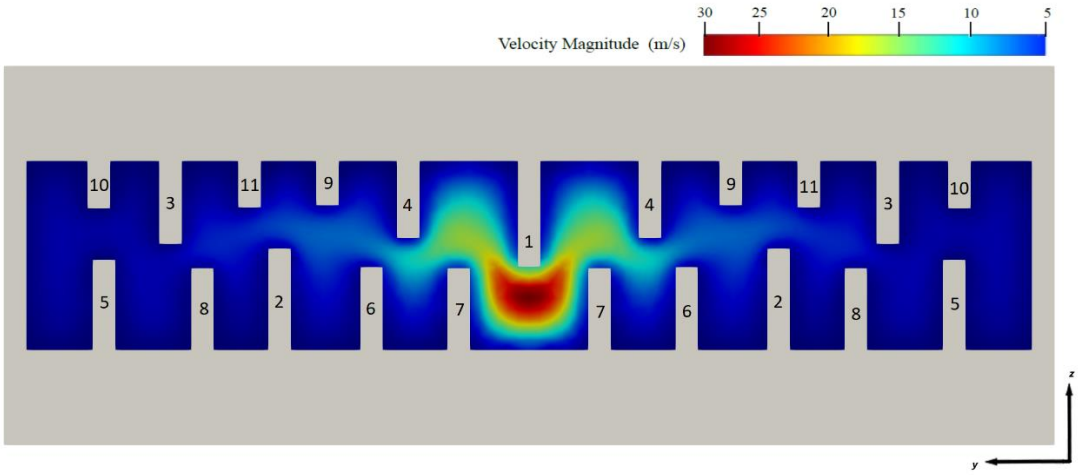

Figure 7. Final fin arrangement on the heat exchanger and velocity profile at the entrance to the domain.

It is also possible to notice from Fig. 7 that fins length decrease during the construction process, i.e., the initially added fins are the longest ones. This is due to the fact that with the change in the internal geometry of the channel, maximum values for the control function are calculated at locations distant from the channel symmetry plane.

Figure 8 presents the isometric view of the heat exchanger focusing on the outlet section of the channel. In this region occurs the largest temperature gradients, being possible to observe how the heat is transferred from the top wall up to the fluid zone, fins and side walls.

In this work, it was decided not to join the upper and lower fins. This may have caused a bad distribution of temperatures between these regions. This may has reduced the contact area between solid and fluid and eventually is not the best option for an optimized heat exchanger. However, this is a preliminary work and further investigations will be necessary to maximize thermal efficiency of the microchannel heat exchanger.

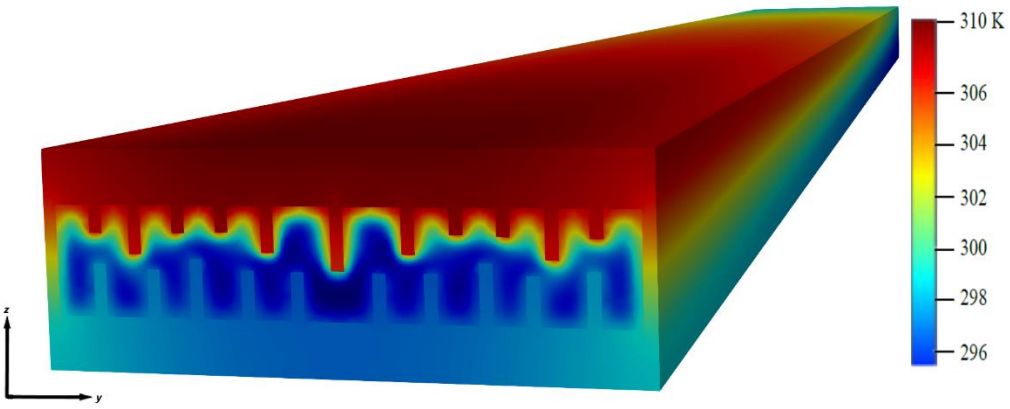

Figure 8. Isometric view of the heat exchanger outlet region.

Figure 9 shows the relationship between the number of fins and the maximum temperatures, Tmax, found in the domain. Stabilization of Tmax was used as the criterion to end the geometry construction process. It is possible to notice a reduction of approximately 20 K, that is, 20 ° C, in the maximum temperatures found between the completely empty channel and the final Constructal form for the channel, representing a reduction of 35% between these values. It is also noticed that from N = 11 there is no great advantage to insert more new fins in the microchannel, showing a sort of saturation of the arrangement.

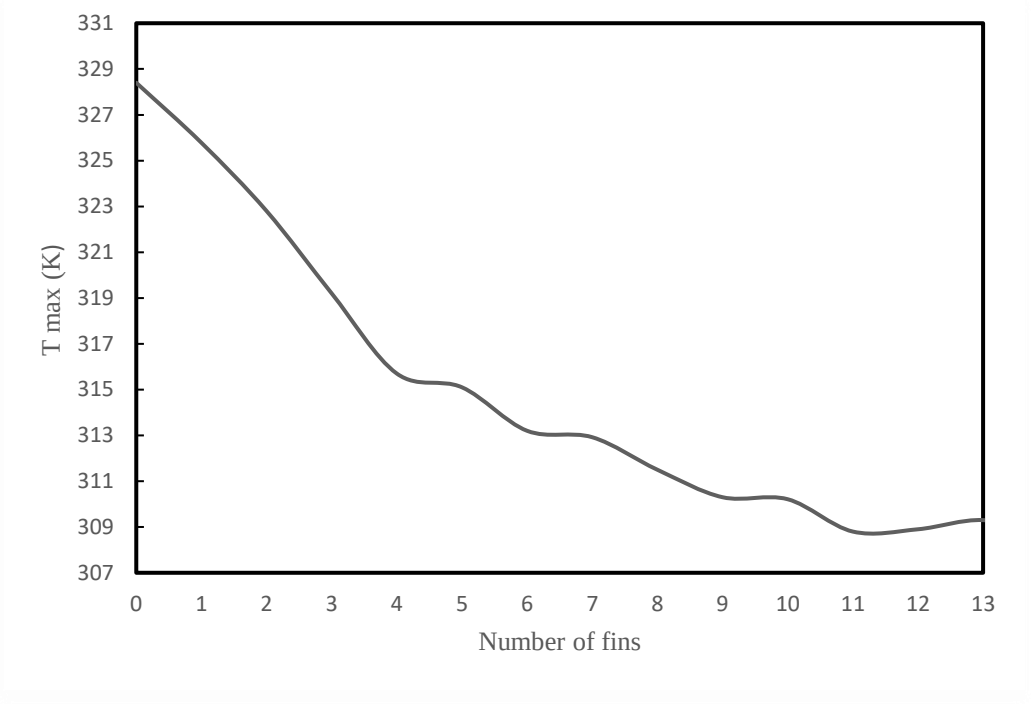

Figure 9. Behavior of the maximum temperature in the domain in relation to the number of fins.

5. CONCLUSIONS

In this work a new microchannel heat exchanger design methodology has been developed. Proposed algorithm is based on Constructal Theory and instead of defining a geometry for the microchannels, internal form of the heat exchanger is made to evolve from a fundamental structure (fin). This paper presents the problem definition, mathematical formulation, numerical solution and the construction algorithm. It is also presented a case study used to validate the CFD solution.

The positioning of the fins proved to be very dependent on the flow velocity. Although it was not necessary to occupy much of the available volume, there was a significant reduction in the maximum temperatures of the domain, requiring a comparative study with a heat exchanger with fins built in the traditional way to evaluate the effectiveness of the method used in this work, in addition to an assessment of the rate of heat transfer between solid and fluid.

The investigation of other conditions, such as different flows to identify if the construction will be similar, may be a point to be analyzed in future works.

6. ACKNOWLEDGMENTS

The author A. M. de Moura acknowledges CAPES for doctorate scholarship (Finance Code 001). J. A. Souza and E. D. dos Santos acknowledge CNPq for research grant (Processes: 304699/2019-5 and 306024/2017-9). All authors thank FAPERGS for financial support in PqG Program – Notice Nº 05/2019 (Process: 19/2551-0001847-9).

7. REFERENCES

Ayachit, U., 2015, The ParaView guide: updated for ParaView version 4.3, (Avila, L.,Ed.), Kitware, Los Alamos, Full color version.

Bejan, A., 1997, “Constructal-theory network of conducting paths for cooling a heat generating volume”, International Journal of Heat and Mass Transfer, Vol. 40, No. 4, pp. 799–816.

Bejan, A., 2000, Shape and structure, from engineering to nature, Cambridge University, Cambridge, UK.

Bello-Ochende, T., Liebenberg, L. and Meyer, J.P., 2007, “Constructal cooling channels for micro-channel heat sinks”, International Journal of Heat and Mass Transfer, Vol. 50, No. 21–22, pp. 4141–4150.

Geuzaine, C. and Remacle, J.-F., 2009, “Gmsh: A 3-D finite element mesh generator with built-in pre- and post-processing facilities”, International Journal for Numerical Methods in Engineering, Vol. 79, No. 11, pp. 1309–1331.

Kawano, K., Sekimuras, M., Minakami, K., Iwasaki, H. and Ishizuka, M., 2001, "Development of Micro Channel Heat Exchanging", JSME International Journal Series B Fluids and Thermal Engineering, Vol. 44, No. 4, pp. 592–598.

Kou, H.-S., Lee, J.-J. and Chen, C.-W., 2008, "Optimum thermal performance of microchannel heat sink by adjusting channel width and height", International Communications in Heat and Mass Transfer, Vol. 35, No. 5, pp. 577–582.

Pedroti, V.A., de Escobar, C.C., dos Santos, E.D. and Souza, J.A., 2020, "Thermal analysis of tubular arrangements submitted to external flow using constructal theory", International Communications in Heat and Mass Transfer, Vol. 111, p. 104458.

Qu, W. and Mudawar, I., 2002a, "Analysis of three-dimensional heat transfer in micro-channel heat sinks", International Journal of Heat and Mass Transfer, Vol. 45, No. 19, pp. 3973–3985.

Qu, W. and Mudawar, I., 2002b, "Experimental and numerical study of pressure drop and heat transfer in a single-phase micro-channel heat sink", International Journal of Heat and Mass Transfer, Vol. 45, No. 12, pp. 2549–2565.

Vianna, J.C.B., Estrada, E. da S.D., Isoldi, L.A., dos Santos, E.D. and Souza, J.A., 2018, "A new Constructal Theory based algorithm applied to thermal problems", International Journal of Thermal Sciences, Vol. 126, pp. 118–124.

Weller, H., Greenshields, C. and de Rouvray, C. (n.d.). "The OpenFOAM Foundation Ltd", OpenFOAM, available at: https://openfoam.org/.

8. RESPONSIBILITY NOTICE

The authors are the only responsible for the printed material included in this paper.